Mars-Van Krevelen cycle and non-noble metal Ni jointly promoting Z-scheme charge transfer: Study on photothermal synergy effect applied in selectively oxidating aromatic alcohols

Gaoli Chen[a], Jing Li[a], Shu Gui[a], Ya Wang[a], Sujuan Zhang[a,*], Zhongliao Wang[a], Xiuzhen Zheng[a], Sugang Meng[a], Chaohui Ruan[a], Shifu Chen[a,*]

[a] Key Laboratory of Green and Precise Synthetic Chemistry and Applications, Ministry of Education, Anhui Province Key Laboratory of Pollutant Sensitive Materials and Environmental Remediation, College of Chemistry and Material Science, Huaibei Normal University, Huaibei, 235000, People's Republic of China.

*Corresponding Authors, Tel: +86-561-3802061, Fax: +86-561-3802061. E-mail: zhangsujuancgl@163.com, chshifu@chnu.edu.cn.

Experimental reagents

Cadmium nitrate tetrahydrate ($Cd(NO_3)_2 \cdot 4H_2O$), thioacetamide (C_2H_5NS), ethylenediamine ($C_2H_4(NH_2)_2$), Cerium nitrate hexahydrate ($Ce(NO_3)_3 \cdot 6H_2O$), sodium hydroxide (NaOH), nickelous nitrate hexahydrate ($Ni(NO_3)_3 \cdot 6H_2O$), Trifluoro toluene (BTF), Deionized water, benzyl alcohol ($C_6H_5CH_2OH$, ≥99.0%), benzaldehyde (C_6H_5CHO, ≥99.0%). All of these are analytical reagents without further purification.

Material characterization

X-ray diffraction (XRD) patterns of the prepared photocatalysts were detected by a Bruker D8 X-ray powder diffractometer using Cu Kα radiation at room temperature. UV-visible diffuse reflection spectra (UV-Vis DRS) were conducted on a TU-1950 Vis-NIR spectrophotometer (TU-1950, Persee) with $BaSO_4$ as a reference. Field emission scanning electron microscopy (FESEM) images were studied on a FEI Quanta 650 scanning electron microscope. The morphologies and microstructures of the photocatalysts were determined by transmission electron microscopy (TEM, FEI Tecnai G2 F20) and high-resolution transmission electron microscopy (HRTEM) at an accelerating voltage of 200 kV, elemental mappings were performed using an

energy-dispersive X-ray spectrometer (EDS) attached to the TEM instrument. X-ray photoelectron spectroscopy (XPS) analysis was performed on an ESCALAB 250 photoelectron spectrometer (Thermo Fisher Scientific) equipped with an Al Ka X-ray beam (1486.6 eV). The binding energies were corrected with reference to the C 1s peak of the surface adventitious carbon at 284.6 eV. The Brunauer-Emmett-Teller (BET) data of the samples was obtained by N_2 adsorption-desorption at 77.3 K using a Micromeritics ASAP 2460 instrument. Photoluminescence (PL) emission spectra were recorded on a JASCO FP-6500 type fluorescence spectrophotometer and time-resolved photoluminescence spectroscopy (TR-PL) was recorded on an Edinburgh FS5 fluorescence spectrophotometer. In situ diffuse reflectance infrared Fourier transform spectroscopy (DRIFT) measurements were performed on a Nicolet 8700 FTIR spectrometer using a KBr window.

The photoelectrochemical tests were implemented on a three-electrode system (CHI-660E, Chenhua Instruments Co., China). A Pt wire and Ag/AgCl were used as the counter electrode and reference electrode, respectively. The sample powder was deposited on the fluoride tin oxide (FTO) substrate to serve as a working electrode. The electrodes were prepared as follows. The 5 mg sample was dispersed in 400 μL of deionized water. Then, the 20 μL slurry was deposited as a film on a 0.5 cm × 0.5 cm FTO substrate. After being dried at room temperature, the working electrode was obtained. Moreover, photocurrent response of the sample was detected in a 0.2 M Na_2SO_4 aqueous solution, EIS Nyquist plots of the samples were detected in 0.1 M KCl solution containing 0.1 M $K_3[Fe(CN)_6]/K_4[Fe(CN)_6]$.

Computational detail:

DFT calculations were conducted through the Vienna ab initio Simulation Package (VASP) with the projector augment wave method. The generalized gradient approximation of the Perdew-Burke-Ernzerhof (PBE) functional was used as the exchange-correlation functional. The cutoff energy was set as 500 eV, and structure relaxation was performed until the convergence criteria of energy and force reached 1×10^{-5} eV and 0.02 eV $Å^{-1}$, respectively. A vacuum layer of 15 Å was constructed to

eliminate interactions between periodic structures of surface models. The van der Waals (vdW) interaction was amended by the zero damping DFT-D3 method of Grimme. The Gibbs free energy was calculated as $\Delta G = \Delta E + \Delta E_{ZPE} - T\Delta S$, where the ΔE, ΔE_{ZPE}, and ΔS are electronic energy, zero-point energy, and entropy difference between products and reactants. The zero-point energies of isolated and absorbed intermediate products were calculated from the frequency analysis. The vibrational frequencies and entropies of molecules in the gas phase were obtained from the National Institute of Standards and Technology (NIST) database.

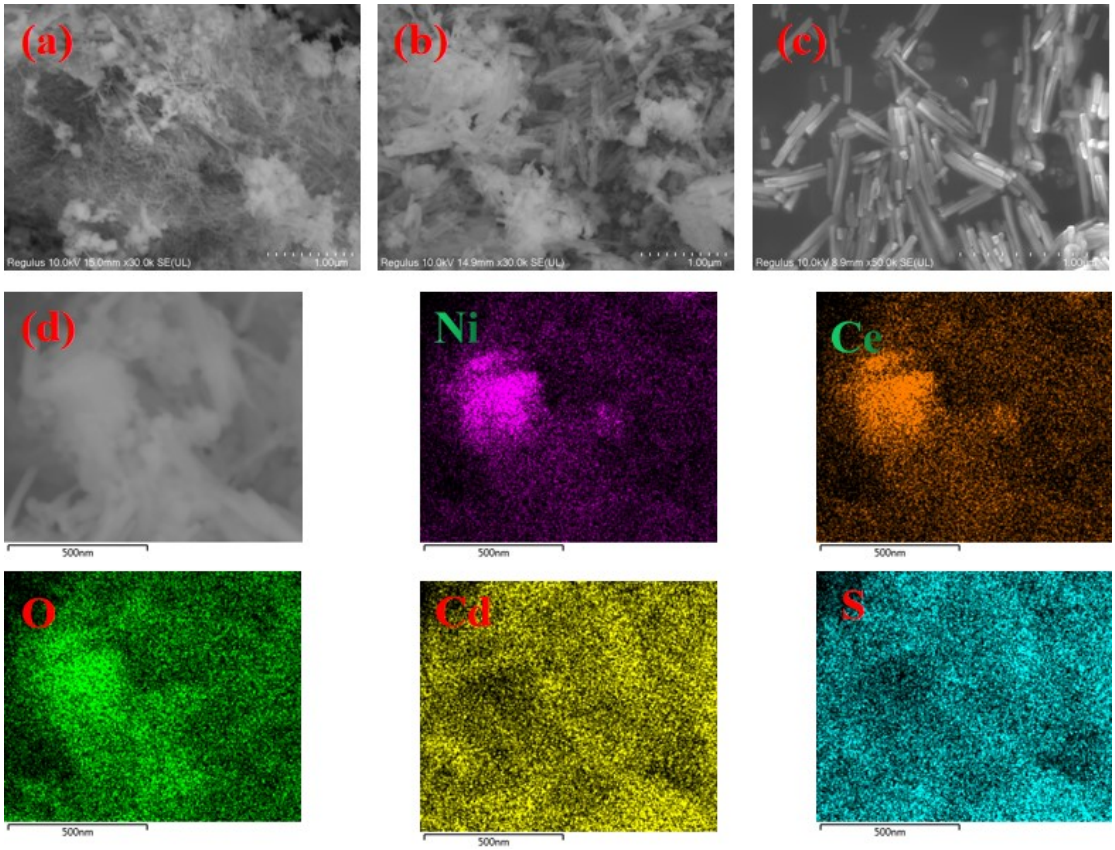

Fig. S1. SEM images of (a) NCO, (b) 60% NCO/CdS, (c) CdS, (d) EDS mapping of 60% NCO/CdS.

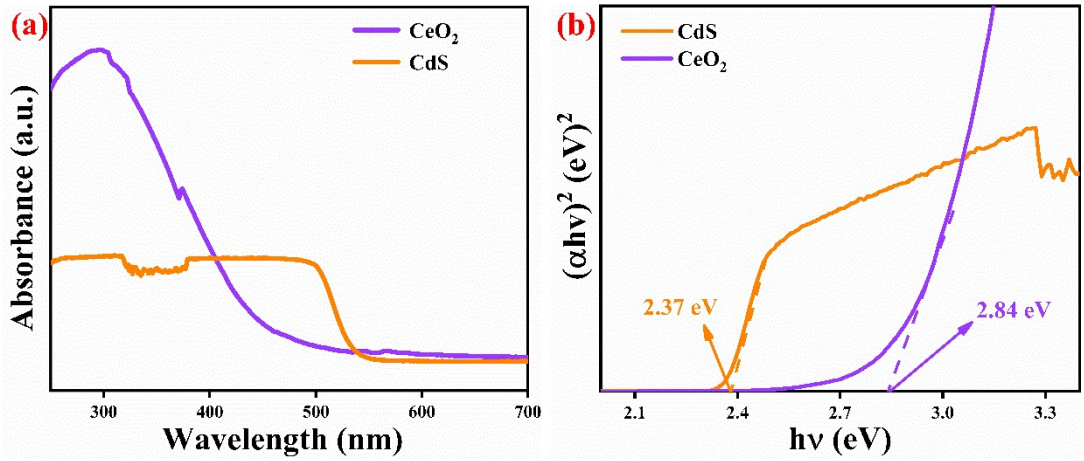

Fig. S2. (a) UV-Vis DRS spectrum, (b) the band gap energy of CeO_2 and CdS.

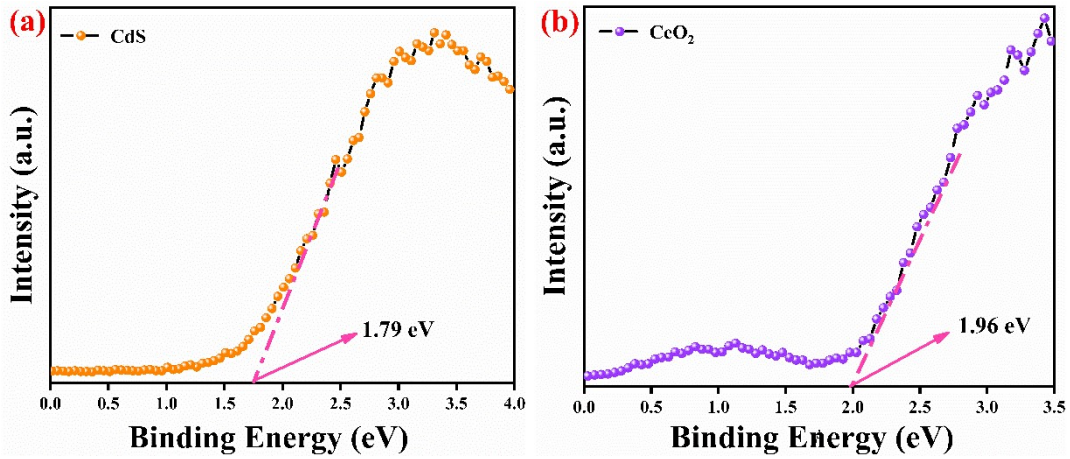

Fig. S3. VB-XPS of (a) CdS, (b) CeO_2.

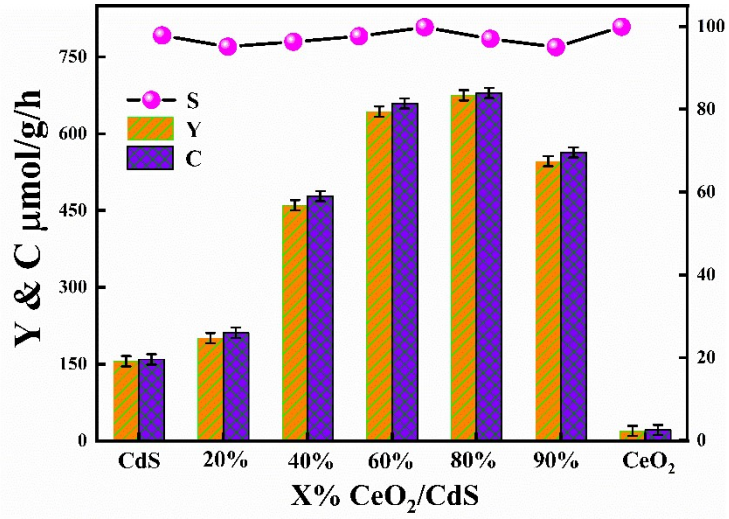

Fig. S4. Catalytic activity of X% CeO_2/CdS.

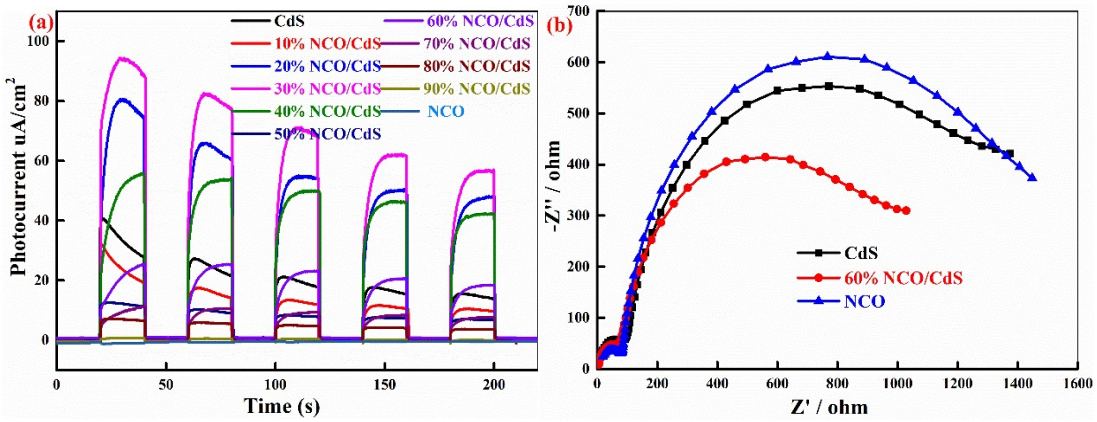

Fig. S5. (a) Photocurrent response of X% NCO/CdS, (b) EIS of X% NCO/CdS.

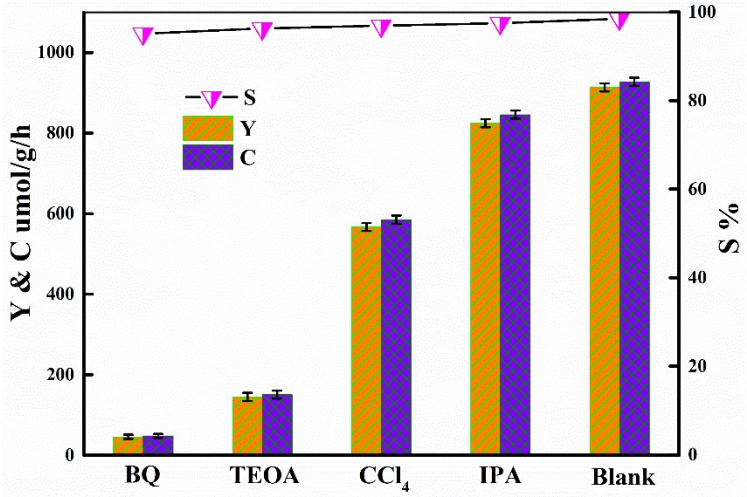

Fig. S6. Catalytic activity of 60% NCO/CdS selective oxidizing benzyl alcohol to benzaldehyde with different scavengers under visible light (363.15 K).

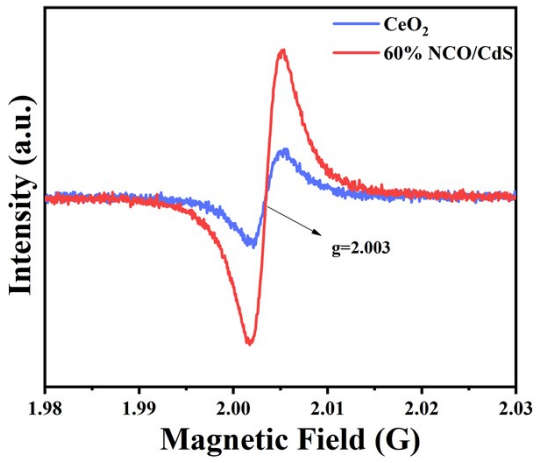

Fig. S7. The EPR results of CeO_2 and 60% NCO/CdS.

Table S1. Reported studies on the selective oxidation of benzyl alcohol.

Catalysts	Reaction solutions	Reaction conditions	Conv. (μmol/g/h)	Sel. (%)	Ref.
g-C_3N_4	50 mg catalyst 10 mL 0.02 mol/L BA/BTF	373 K, 0.1 Mpa O_2, 4 h	230	98	[1]
Bi_2MoO_6	16 mg catalyst 0.1 mmol BA, 1.5 mL BTF	298 K, 0.1 Mpa O_2, 4 h	414.06	>99	[2]
10% Mn_3O_4/ $Cd_{0.9}Zn_{0.1}S$	100 mg catalyst 15 mL 0.02 mol/L BA/BTF	353 K, 0.1 Mpa O_2, 4 h	377.25	100	[3]
50% Cr_2O_3- Al_2O_3/CdS	100 mg catalyst 15 mL 0.038 mol/L BA/BTF	353 K, 0.1 Mpa O_2, 4 h	742.43	99	[4]
$CdIn_2S_4$	80 mg catalyst, 15 mL 0.0255 mol/L BA/BTF	333 K, 0.1 Mpa N_2, 4 h	689.69	83.6	[5]
CdS/ g-C_3N_4	100 mg catalyst, 15 mL 0.0255 mol/L BA/BTF	333 K, 0.1 Mpa N_2, 4 h	426.48	93	[6]
60% NCO/CdS	100 mg catalyst 15 mL 0.038 mol/L BA/BTF	363.15 K, atmospheric pressure, 4 h	913.45	100	This work

[1] L. Zhang, D. Liu, J. Guan, X. Chen, X. Guo, F. Zhao, T. Hou and X. Mu, Mater. Res. Bull., 2014, 59, 84–92.

[2] K. Jing, J. Xiong, N. Qin, Y. Song, L. Li, Y. Yu, S. Liang and L. Wu, Chem. Commun., 2017, 53, 8604–8607.

[3] S. Gui, S. Zhang, G. Chen, Z. Zhu, X. Zheng, S. Meng, C. Ruan and S. Chen, Appl. Surf. Sci., 2021, 579, 151978.

[4] S. Meng, S. Chang and S. Chen, ACS Appl. Mater. Interfaces, 2020, 12, 2531–2538.

[5] X. Ye, Y. Chen, C. Ling, R. Ding, X. Wang, X. Zhang and S. Chen, Dalton Trans., 2018, 47, 10915–10924.

[6] X. Ye, X. Dai, S. Meng, X. Fu and S. Chen, Chinese J. Chem., 2017, 35, 217–225.

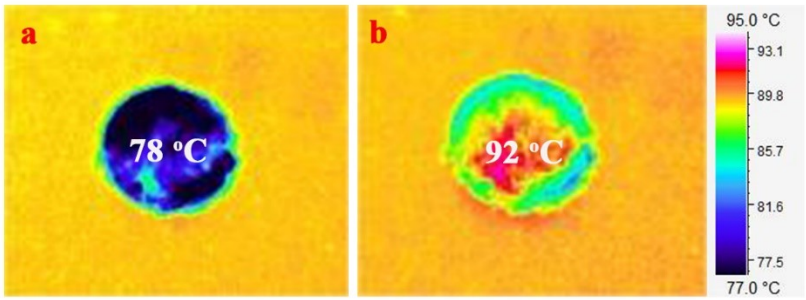

Fig. S8 Surface temperatures of 60% NCO/CdS (heating platform: 363.15 K (90 ℃)): (a) without illumination, (b) illumination. Orange background is the temperature (about 90 ℃) of the heating platform.

CdS (001)

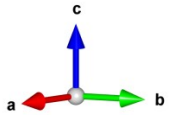

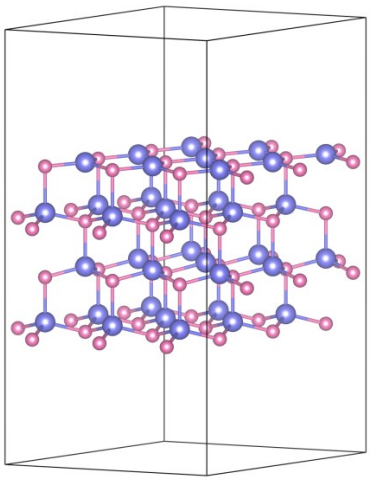

CeO_2 (111)

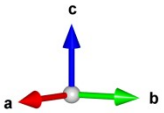

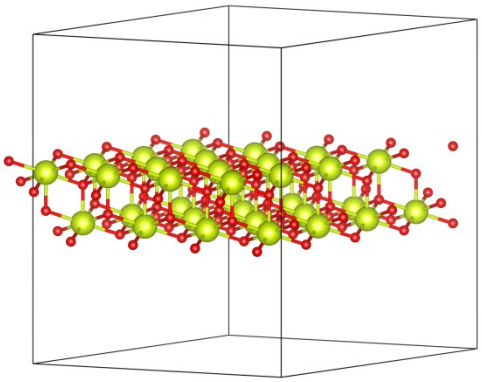

Ni (111)